

Low-Cost Synthesis of Highly Luminescent Colloidal Lead Halide Perovskite Nanocrystals by Wet Ball Milling

Loredana Protesescu, Sergii Yakunin, Olga Nazarenko, Dmitry N Dirin, and Maksym V. Kovalenko

ACS Appl. Nano Mater., **Just Accepted Manuscript** • DOI: 10.1021/acsanm.8b00038 • Publication Date (Web): 05 Mar 2018

Downloaded from <http://pubs.acs.org> on March 6, 2018

Just Accepted

“Just Accepted” manuscripts have been peer-reviewed and accepted for publication. They are posted online prior to technical editing, formatting for publication and author proofing. The American Chemical Society provides “Just Accepted” as a service to the research community to expedite the dissemination of scientific material as soon as possible after acceptance. “Just Accepted” manuscripts appear in full in PDF format accompanied by an HTML abstract. “Just Accepted” manuscripts have been fully peer reviewed, but should not be considered the official version of record. They are citable by the Digital Object Identifier (DOI®). “Just Accepted” is an optional service offered to authors. Therefore, the “Just Accepted” Web site may not include all articles that will be published in the journal. After a manuscript is technically edited and formatted, it will be removed from the “Just Accepted” Web site and published as an ASAP article. Note that technical editing may introduce minor changes to the manuscript text and/or graphics which could affect content, and all legal disclaimers and ethical guidelines that apply to the journal pertain. ACS cannot be held responsible for errors or consequences arising from the use of information contained in these “Just Accepted” manuscripts.



Low-Cost Synthesis of Highly Luminescent Colloidal Lead Halide Perovskite Nanocrystals by Wet Ball Milling

Loredana Protesescu,^{†,‡,*} Sergii Yakunin,^{†,‡} Olga Nazarenko,^{†,‡} Dmitry N. Dirin,^{†,‡} and Maksym V. Kovalenko^{†,‡,*}

[†] Institute of Inorganic Chemistry, Department of Chemistry and Applied Bioscience, ETH Zürich, Vladimir Prelog Weg 1, CH-8093 Zürich, Switzerland

[‡] Laboratory for Thin Films and Photovoltaics, Empa – Swiss Federal Laboratories for Materials Science and Technology, Überlandstrasse 129, CH-8600 Dübendorf, Switzerland

KEYWORDS: lead halide perovskite, nanocrystals, photoluminescence, mechanochemical synthesis, ball milling.

ABSTRACT. Lead halide perovskites of APbX₃ type [A = Cs, formamidinium (FA), methylammonium (MA); X = Br, I] in the form of ligand-capped colloidal nanocrystals (NCs) are widely studied as versatile photonic sources. FAPbBr₃ and CsPbBr₃ NCs have become promising as spectrally narrow green primary emitters in backlighting of liquid-crystal displays (peak at 520–530 nm, full width at half maximum of 22–30 nm). Herein, we report that wet ball milling of bulk APbBr₃ (A=Cs, FA) mixed with solvents and capping ligands yields green

luminescent colloidal NCs with a high overall reaction yield and optoelectronic quality on par with that of NCs of the same composition obtained by hot-injection method. We emphasize the superiority of oleylammonium bromide as a capping ligand used for this procedure over the standard oleic acid and oleylamine. We also show a mechanically induced anion-exchange reaction for the formation of orange-emissive CsPb(Br/I)₃ NCs.

1. INTRODUCTION

Bottom-up synthesis methods of surfactant (ligand)-capped colloidal nanocrystals (NCs), such as high-temperature hot injection or heating methods, have afforded an unprecedented variety of NC compositions and morphologies, with a high level of uniformity and narrow size distribution.¹⁻⁵ Colloidal synthesis in apolar solvents has enabled the development and recent commercial applications of colloidal semiconductor NCs (also known as quantum dots, QDs) composed of typical binary compound semiconductors: II-VI (CdS, CdSe, CdTe),¹ III-V (InP, InAs, InSb),⁶⁻⁹ and IV-VI (PbS, PbSe, PbTe).¹⁰⁻¹⁹ In addition, QDs with high structural complexity have been achieved, with the most notable examples being core-shell QDs (CdSe/ZnS^{5,20} and PbX/CdX,²¹⁻²³ X = S, Se, Te), nanowires,²⁴ nanodisks,²⁵ nanoplatelets (NPLs),²⁶ rods and tetrapods.²⁷

Unsurprisingly, the most recent addition to the family of colloidal QDs, NCs of lead halide perovskites [LHPs; APbX₃-type; A = Cs, formamidinium (FA), methylammonium (MA); X = Br, I] were initially approached with the same experimental mindset.²⁸ For example, the first synthesis of CsPbX₃ NCs was accomplished by injecting a Cs precursor into a PbX₂ solution at elevated temperatures.²⁹ Similarly, highly luminescent FA- and MA-based LHPs were synthesized by injecting the sources of MA and FA cations.³⁰⁻³¹ Colloidal Cs- and FA-based

LHP NCs^{29, 31-32} exhibit broadly tunable photoluminescence (PL), spanning the entire visible spectral range (410–700 nm), small PL linewidths (full width at half maximum, FWHM, 12–40 nm for blue-to-red), and high PL quantum yields (QYs, 50%–90%), thus providing a broad color gamut.

LHPs are ionic and are characterized by low formation and lattice energies; therefore, they do not require thermal activation during formation to achieve high crystallinity. Subsequent studies have shown that the synthesis of colloidal LHP NCs involves a surfactant-controlled coprecipitation of ions that proceeds with fast kinetics even at room temperature (RT). Facile formability of LHP NCs has been successfully achieved using an alternative strategy, the reprecipitation method, wherein an ionic solution of the respective ions (A^+ , Pb^{2+} , and X^-) in a polar solvent is rapidly destabilized by mixing with a non-solvent, inducing a burst of nucleation. This method was originally proposed for $MAPbBr_3$ NCs³³ and has since been extended to Cs and FA systems. Non-cuboidal shapes, such as NPLs, nanosheets, and nanowires, can also be obtained using both methods.³⁴⁻³⁷

The soft nature of LHPs and their facile crystallization suggest that top-down methods might also be applicable for LHP NC preparation. In this study, we report a simple mechanochemical synthesis of LHP NCs using a commercial ball mill. Such a synthesis essentially involves simple mechanical grinding of bulk $APbX_3$ materials or $AX + PbX_2$ mixtures in the presence of a solvent (mesitylene) and ligand (oleylammonium halide, OAmX, or mixture of oleic acid, OA, and oleylamine, OLA). These ligands are chosen based on their success in hot-injection synthesis methods.^{29, 31}

High-energy ball milling is a type of mechanical grinding of materials. This process can be conducted in a dry (without solvents) or wet (with solvents) fashion. Laboratory-scale ball

milling (5–100 mL scale) is a batch process, whereas industrial ball mills can be operated in a continuous mode, thus offering a very high synthesis throughput. The milling occurs due to mechanical friction between the grinding medium, such as balls of the same or various sizes, and the ground material (Figure 1). The container (bowl) and the grinding balls are typically made of the same, high-hardness material (zirconia, corundum, or stainless steel). Mechanical energy is provided to the system by the rotary motion of the bowl, as in the case of a planetary ball mill. The rotation of the bowl and the speed are optimized such that the maximum speed, the speed at which balls do not move within the bowl, is not exceeded. The milling can have diverse effects on the ground material: different extents of downsizing of the final powder (from microns to tens of nanometers), efficient mixing (e.g., production of slurries in battery manufacturing or preparation of pigments), solid-state chemical transformation (mechanochemical synthesis), or a combination of these effects.³⁸⁻³⁹ Wet ball milling is also considered to be a green chemistry approach, as it does not require high temperatures (energy saving) and consumes minimal quantities of solvents.⁴⁰ Ball milling has been popular since the 1970s for producing oxide dispersions such as Al_2O_3 , Y_2O_3 , and ThO_2 . Grinding techniques are also widely used for alloying materials,⁴¹ in the synthesis of metal oxides,^{39, 42-43} and for mechanical exfoliation of graphene.⁴⁴ However, in terms of the synthesis of semiconductor NCs, ball milling has achieved very limited success (examples include CdSe ⁴⁵ and CdTe ⁴⁶) due to the lack of bright emission from the resulting QDs. This is because, on the one hand, ball milling generates numerous structural defects in rigid lattices of these materials, and on the other hand, it does not allow surface passivation. The combined effect of the trap states, which are abundant on the pristine (uncoated) NC surfaces, and other structural defects leads to very low PL QYs. Therefore, it is necessary to coat conventional QDs with wide-bandgap materials, such as in the canonical

example of core-shell CdSe-CdZnS NCs, thereby decoupling the excitonic recombination from the detrimental surface states.

On the contrary, LHP NCs are unique in that they do not require surface passivation with epitaxial wide-bandgap semiconductor layers for exhibiting bright emission in the green-red spectral region. This is one of the manifestations of the rare phenomenon of defect tolerance: structural defects are nearly fully benign with respect to the carrier dynamics. Theoretical calculations indicate that dominant point defects, primarily vacancies, in the bulk material,⁴⁷ at grain boundaries,⁴⁸ and on the NC surfaces⁴⁹ are all shallow or intra-band (in the valence or conduction bands). Other defects, for instance, those of the antisite or interstitial type, are not common in perovskites due to their crystal structure and ionic bonds. Defect tolerance makes LHPs vastly different from all known types of colloidal QDs and enables many synthesis pathways for LHP NCs. Besides the mechanochemical synthesis presented here and by others (see further discussion in the next section),⁵⁰⁻⁵¹ perovskite NCs with bright PL were obtained by sonication,⁵² microwave irradiation,⁵³⁻⁵⁴ or templating of crystallization using the nanoscale pores of mesoporous silica.⁵⁵

2. RESULTS AND DISCUSSION

The goal of this study was to produce highly luminescent CsPbBr₃ and FAPbBr₃ NCs in one step by ball milling. Both of these nanomaterials can be readily synthesized on microfluidic platforms⁵⁶ and by the hot-injection colloidal method,^{29, 31, 57-58} ultrasonication,⁵² the re-precipitation method at RT,⁵⁹⁻⁶⁰ and microwave-assisted growth.^{53-54, 61} Mechanochemical syntheses were initially used only for MAPbI₃,^{51, 62} wherein relatively large micro- and nanoparticles (>200 nm) are formed on Al₂O₃ carrier particles. In a recent report,⁵⁰ dry ball

1
2
3 milling of CsX and PbX₂ powders followed by the addition of OLA yielded luminescent
4
5 colloidal NCs. In our own experiments, we were unable to produce stable and bright colloids
6
7 with only OLA as the ligand. Also, dry-milling was ineffective in our experiments, irrespective
8
9 of the ligands used afterwards or whether bulk APbX₃ or AX+PbX₂ mixtures were used as
10
11 starting precursors. Below, we detail our own study, wherein different ligand systems were used:
12
13 (i) a mixture of OLA and OA and (ii) OAmX. These ligand systems were previously used in
14
15 mostly all colloidal syntheses of perovskite NCs and the general consensus was that OAm⁺
16
17 coordinates the surface anions, whereas Br⁻ or oleate anions locate themselves close to surface
18
19 cations, thereby maintaining the overall charge neutrality of the NC.^{49, 63-64}
20
21
22
23

24 The ball-milling method (Figure 1) employs two rotational movements: one of the milling
25
26 bowl and the other of the supporting disk (on which the bowl with NCs is mounted). The
27
28 combined effect enables the efficient movement of the balls within the bowl, causing grinding of
29
30 the material. If only circular motion of the bowl was employed, such as in centrifuges, all
31
32 components of the mixture would be statically held by the centrifugal force. As precursor
33
34 materials, either a bulk APbX₃ compound or an equimolar mixture of AX and PbX₂ is used. The
35
36 combined effect of milling and the presence of the capping ligands and solvents allows for a
37
38 simple one-step conversion of bulk precursors into colloids of APbX₃ NCs. The optimal milling
39
40 time at RT and 500 rpm is dependent on the material: 2 h for CsPbBr₃ and 1 h for FAPbBr₃.
41
42
43

44 In a typical experiment (see Experimental section for the detailed protocols), 0.035 mmol of
45
46 CsPbBr₃ or 0.04 mmol of FAPbBr₃ was loaded into a zirconia bowl with 25 zirconia balls (4 mm
47
48 and 5 mm in diameter). OAmBr (0.03 mmol) was added as the ligand and 0.4 mL of mesitylene
49
50 was added as the solvent. The milling speed was set to 500 rpm and milling time to 2 h (for
51
52 CsPbBr₃) and 1 h (for FAPbBr₃), as found to be optimal for obtaining NCs (Figure 2b). Powder
53
54
55
56
57
58
59
60

X-ray diffraction (XRD) patterns confirmed the complete conversion of the precursors into nanogranular products with the expected crystal structure (orthorhombic for CsPbBr₃ and cubic for FAPbBr₃).

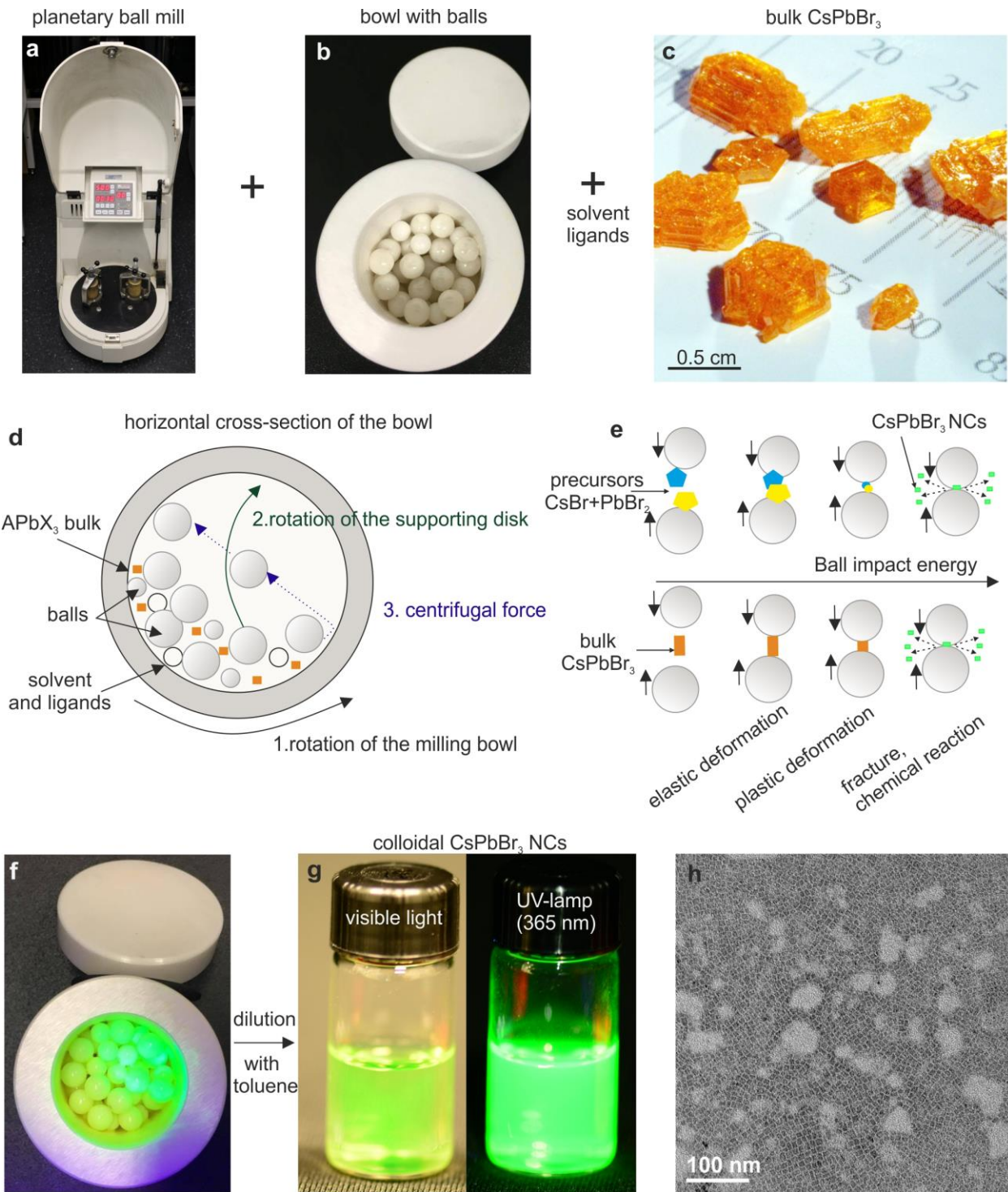


Figure 1. Photographs of (a) a typical planetary ball mill, (b) zirconia bowl filled with zirconia balls, and (c) crystals of bulk CsPbBr₃ used as starting materials. (d) Schematic of the working principle of the planetary ball mill showing the horizontal cross-section of the bowl during the wet ball-milling experiments. The bowl undergoes two motions: orbital rotation of the entire ball and its simultaneous spinning. (e) Schematic of the processes occurring during the mechanochemical synthesis of LHP NCs. Photographs showing the colloid of CsPbBr₃ NCs (f) directly after the ball-milling experiment and (g) after dilution with toluene and filtration (taken under visible light and under a UV lamp, $\lambda = 365$ nm). (h) TEM image of the resulting CsPbBr₃ NCs.

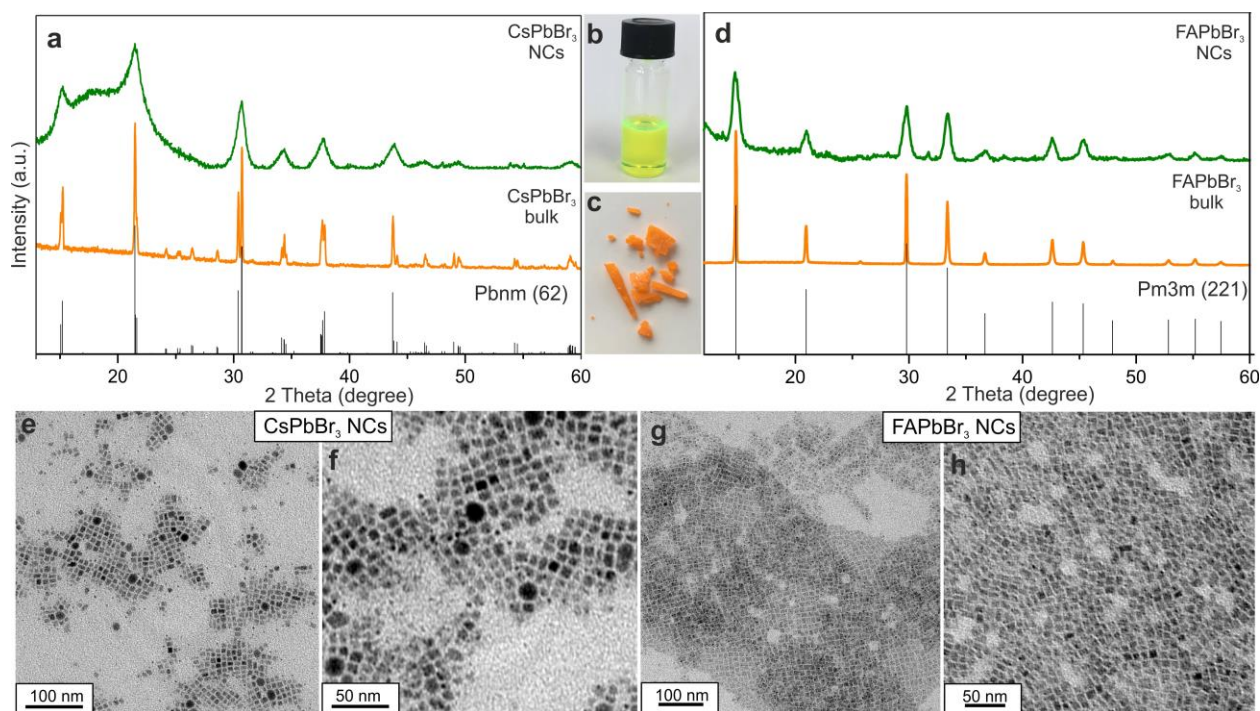


Figure 2. (a) Powder XRD patterns of bulk CsPbBr₃ (orange pattern) used for the ball-milling experiment, and the resulting CsPbBr₃ NCs (green pattern) showing an identical orthorhombic perovskite crystal structure (*Pnma* space group); (b) photograph showing the obtained colloidal CsPbBr₃ NCs diluted in toluene; (c) photograph showing the initial bulk CsPbBr₃ crystals; (d) comparison of the XRD patterns of bulk FAPbBr₃ (orange pattern) used for the ball-milling experiment and the resulting FAPbBr₃ NCs (green pattern), indicating the retention of the cubic lattice; (e–h) TEM images of CsPbBr₃ NCs and FAPbBr₃ NCs at various magnifications.

The ball-to-material weight ratio, wherein “material” is the mixture of precursors, ligands, and solvents, is an important parameter for obtaining uniform NCs: the higher the ratio, the shorter

the time required for complete milling of the bulk materials. A broad range for this parameter is reported in the literature for various materials (from 1 to 220).^{38, 65-66} By keeping the number of balls constant and changing the amount of material, the ball-to-material ratio was varied from 21.7 to 167 (Figure S1). The optimal ball-to-material weight ratio was found to be 80 [approx. 10 balls (4 mm) and 15 balls (5 mm), 0.035 mmol CsPbBr₃ (0.04 mmol for FAPbBr₃), 0.1 g OAmBr, 0.4 mL mesitylene], yielding PL FWHM = 27 nm for CsPbBr₃ NCs (PL peak at 510 nm) after 2 h of milling. Very long milling times often caused the emergence of mixed shapes, in particular, a large fraction of NPLs. NPLs were apparent in the blue-shifted bands in the PL spectra (Figure S2a, Figure S4). For example, for FAPbBr₃, NCs with an emission peak at 537 nm could be readily obtained within 1 h (Figure 3a). A longer milling (*ca.* 2 h) time led to the appearance of an emission peak at 450 nm. This band was dominant in the PL spectrum after 3 h (Figure S2b). OAmBr was the most suitable ligand for both perovskite materials, giving stable colloidal dispersions and narrow emission linewidths. When only OLA was used, no NCs were formed (no PL was observed), whereas using OA as the sole ligand yielded bright suspensions but unstable colloids with fast decay of the PL QY upon storage. A mixture of OA and OLA allowed the fabrication of stable colloids of FAPbBr₃, but with broader PL linewidths (Figure S3b, FWHM = 34 nm) most likely due to acid/base equilibrium reactions between the ligands, therefore the existence of protonated and unprotonated species in the same time increased the probability to obtain NCs with a broader size distribution. The attempts to form CsPbBr₃ NCs with OA and OLA resulted in a mixture of NCs and NPLs (Figure S3a). Other ligands, such as tetraoctylammonium bromide, induced the formation of bright FAPbBr₃ NCs but without satisfactory colloidal stability (Figure S3). Mesitylene was identified as the best solvent for colloidal stability; other tested solvents included octadecene, toluene, diphenyl, hexane, and

chloroform. Dry milling, e.g. without solvents and ligands, leads only to poorly luminescent microcrystalline powders.

Time-resolved PL traces of both CsPbBr₃ and FAPbBr₃ samples were characterized by multi-exponential decay behavior (Figure 3b). This could be explained by the broad size and shape distribution of the NCs after ball milling. This was also consistent with the broader emission band observed for NCs obtained by ball milling than for NCs obtained by hot injection.²⁹ For CsPbBr₃ NCs, the fastest decay component in the bi-exponential fitting model was at least two times longer than nearly monoexponential decay parameter for NCs produced by hot injection (10.6 vs. 5 ns). FAPbBr₃ NCs, however, showed notably faster relaxation times than colloiddally synthesized NCs of the same composition.³¹ We associate this to the larger fraction of smaller NCs in the ball-milled FAPbBr₃ product. In smaller NCs, higher quantum confinement accelerates the radiative rate. The acceleration due to surface states (the effect is rather common for II-VI QDs) can be ruled out by the observation of PL QYs. PL QYs were high and similar in solutions (>75% for CsPbBr₃ NCs, >80% for FAPbBr₃ NCs). Films of FAPbBr₃ NCs nearly retained their high PL QYs (>70%), whereas CsPbBr₃ NC films exhibited a significant decrease to 45% (Figure 3c). High initial QY and better stability in film for FAPbBr₃ NCs can be attributed to the better tolerance to defects, lower density of defects and also higher defect formation energy.⁶⁷ In films of FAPbBr₃ NCs, the relaxation speed was slower than in the solution, as opposed to CsPbBr₃ NC where relaxation is slightly faster than in the corresponding solution (Figure 3d). Such different behavior of NC with organic and inorganic cations can be explained by the higher tendency of FAPbBr₃ NCs to sintering at room-temperature (bulk material has lower melting point) and higher density of surface defects in CsPbBr₃ with lower defect formation energy.⁶⁸

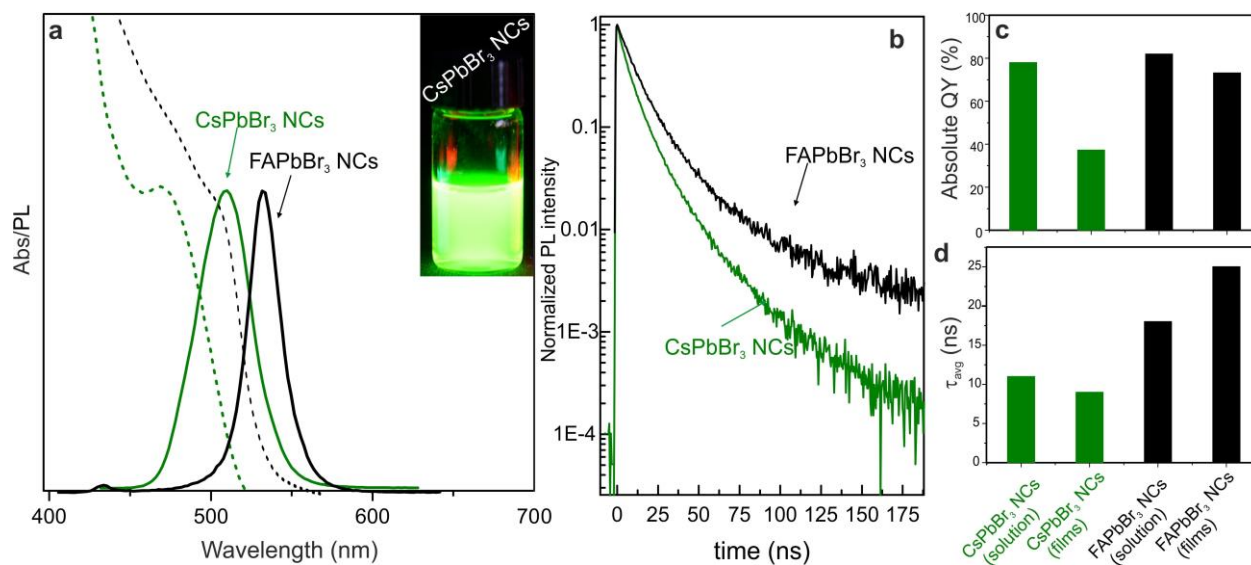


Figure 3. (a) Absorbance and PL spectra for CsPbBr₃ NCs (green) and FAPbBr₃ NCs (black) obtained using the ball-milling method, inset: photograph of CsPbBr₃ NCs under UV lamp ($\lambda = 365$ nm), (b) time-resolved PL of CsPbBr₃ NCs (green) and FAPbBr₃ NCs (black) measured in solutions, (c) absolute QY of CsPbBr₃ NCs (green) and FAPbBr₃ NCs (black) measured in solutions and films, and (d) decay time for CsPbBr₃ NCs (green) and FAPbBr₃ NCs (black) measured in solutions and films.

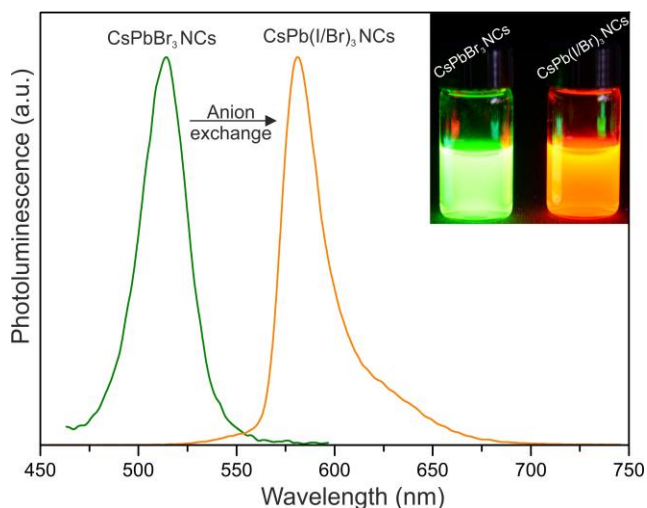


Figure 4. Example of an anion-exchange reaction performed by adding OAmI to the bowl immediately after the synthesis of CsPbBr₃ NCs (520 nm). Within several minutes, the PL peak shifted from 520 nm to 580 nm, indicating the formation of CsPb(Br/I)₃ NCs.

Attempts to compositionally tune the bandgap by methods such as milling bulk CsPbBr₃ and oleylammonium iodide (OAmI) as starting materials showed limited success, as the resulting NCs exhibited low PL QYs. A better approach was to conduct an anion-exchange reaction³² by adding OAmI to CsPbBr₃ NCs (Figure 4).

The results of the mechanochemical synthesis using CsBr and PbBr₂ as precursors are illustrated in Figure 5 and compared with those of the identical procedure using the CsPbBr₃ precursor. Even after 14 h, the FWHM of the obtained NCs was 49 nm (centered at *ca.* 500 nm), indicating that it was very important to use a bulk ternary compound as a precursor rather than the mixture of two binary. Using two precursors, we can expect two simultaneous phenomena: the mechanical downsizing of the precursors and the chemical reaction between CsBr and PbBr₂; the nucleation of CsPbBr₃ NCs could be initiated any time during those processes and therefore different NCs will have different growth history., yielding polydisperse ensemble or remanence of some bulk material. If a shorter ball-milling reaction time is considered (1 h), the obtained NCs with emission at 522 nm and FWHM of 27 nm, were not colloidally stable. This suspension contained most of the material in the non-luminescent bulk phase. After centrifuging and filtering, only a highly dilute colloid was obtained (≤ 1 mg/mL, $< 5\%$ of theoretical reaction yield). Hence, the narrow PL band could be attributed to the strong reabsorption of PL by the bulk material. Unbalanced kinetics of the formation of new NCs and downsizing of the earlier formed NCs eventually led to a very broad PL peak.

Finally, we would like to point that this ball-milling synthesis method was essentially inapplicable to iodide systems (CsPbI₃ and MAPbI₃, Figure S5).

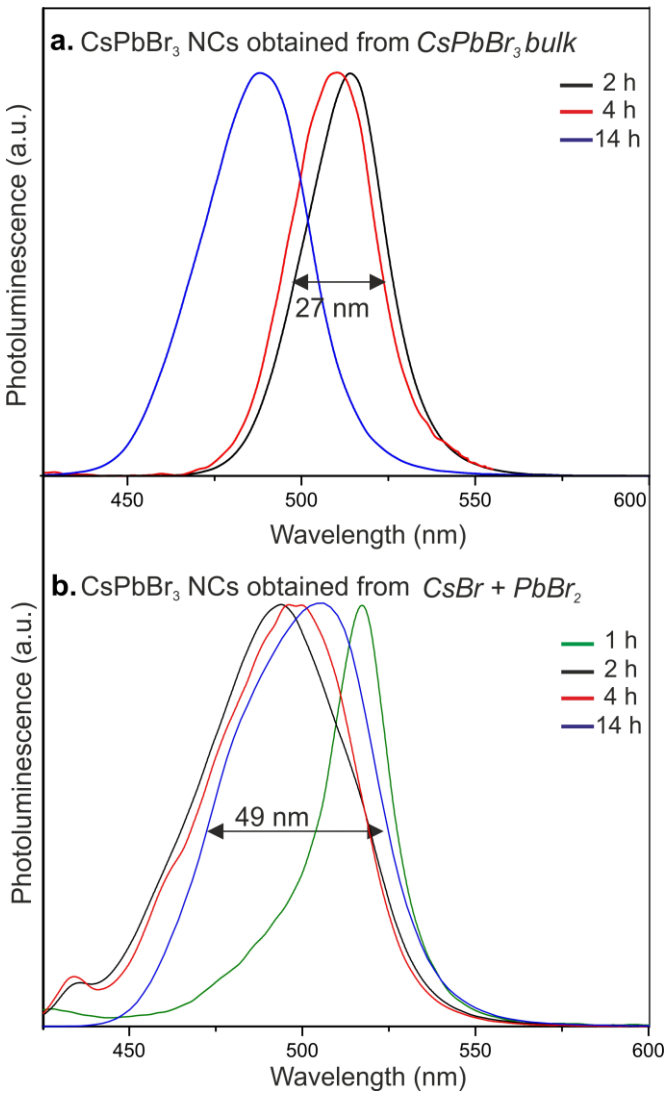


Figure 5. Comparison between ball-milling synthesis of CsPbBr₃ NCs employing bulk CsPbBr₃ and that employing a mixture of CsBr and PbBr₂ as precursors.

3. CONCLUSIONS

In summary, this study explored the utility of wet mechanical grinding for obtaining colloidal NCs of lead halide perovskite. The method yielded FAPbBr₃ and CsPbBr₃ NCs with optoelectronic quality on par with that required for application in the backlighting of liquid-

crystal displays (as the green primary color). The utmost simplicity and speed of mechanochemical synthesis indicated its utility for future research. For instance, the fast downsizing achieved by this synthesis could be used as a general method for testing whether certain bulk materials, such as soft metal halides, can become bright emitters in the form of NCs.

4. METHODS

Synthesis of bulk CsPbBr₃, adapted from Ref.⁶⁹ Bulk CsPbBr₃ crystals were obtained from dimethylsulfoxide (DMSO, 99.8%, Fluka) solution at 110 °C. First, CsBr (Aldrich, 99.9%) and PbBr₂ (99.999%, ABCR) were dissolved in DMSO with [Cs] and [Pb] of 0.5 M and 1 M, respectively. This solution was filtered at RT and then slowly heated to 110 °C. Typically, numerous sub-millimeter crystals appeared just above 90 °C and continued to grow with increasing temperature. After ~4 h of growth, the crystals were taken out of the solution, wiped with filter paper to remove the solvent, and dried overnight in a vacuum oven at 50 °C.

Synthesis of bulk FAPbBr₃. FA acetate (3.2 mmol, 0.33 g, Aldrich, 99%) was dissolved in 1 mL HBr (48%, aqueous solution, Aldrich). PbBr₂ (3.2 mmol, 1.174 g, 99.99%, Aldrich) was dissolved in 2 mL HBr, and this solution was heated to 80 °C to fully dissolve the salts. To this warm solution, the FA solution was added, forming a red precipitate. The mixture was cooled to RT and centrifuged. The precipitate was rinsed with diethyl ether several times to remove the residual acid and dried on a filter paper.

Synthesis of bulk MAPbI₃, adapted from Ref.⁷⁰ Pb(OAc)₂·3H₂O (11.33 mg, 0.03 mmol, ≥99.99%, Aldrich) was dissolved in 38.7 mL hydroiodic acid (HI, 57 wt%, stabilized with 1.5% H₃PO₂, ABCR or Aldrich) and heated to 100 °C in an oil bath. Then, a mixture of 2.52 g methylamine aqueous solution (40 wt%, Fluka) and 8.45 mL of HI was added. Small-grained

black powder precipitated within a few minutes. Then, the solution was cooled to 75 °C and maintained at this temperature for 1 day. The obtained powder was washed with diethyl ether and dried in vacuum at 25 °C.

*Preparation of oleylammonium halide (OAmX).*³² Ethanol (100 mL, Aldrich, absolute, >99.8%) and OLA (12.5 mL, Acros Organics, 80%–90%) were combined in a 250 mL two-necked flask and vigorously stirred. The reaction mixture was cooled in an ice-water bath and 8.56 mL HBr (48% aqueous solution, Aldrich) for preparing OAmBr or 10 mL HI (HI 57%, Aldrich, no stabilizer) for preparing OAmI was added. The reaction mixture was left to react overnight under N₂ flow. Then, the solution was dried under vacuum and the obtained product was purified by rinsing several times with diethyl ether. The product (white powder) was obtained after vacuum-drying at 80 °C overnight.

Mechanochemical synthesis of CsPbBr₃ NCs. Bulk CsPbBr₃ (0.02 g, 0.035 mmol, prepared as described above) was loaded into a zirconia bowl with 25 zirconia balls (4 mm and 5 mm) and with OAmBr (0.01 g, 0.03 mmol, prepared as described above), and 0.4 mL of mesitylene (98%, Sigma-Aldrich). Another tested ligand system was a mixture of OA (0.05 mL, Sigma-Aldrich, 90%) and OLA (0.05 mL, Strem, 95%). Other tested solvents were octadecene (Sigma-Aldrich, 90%), Dowtherm A (diphenyl, eutectic mixture of 26% diphenyl + 73.5% dipheniloxide), toluene (Sigma-Aldrich, 99.5%), hexane (>95%, Sigma-Aldrich), and chloroform (HPLC grade, Fisher Chemicals). The bowl was mounted on a planetary ball mill (Fritsch, Pulverisette 7, classic line) and the speed was set to 500 rpm. The time was varied from 30 min to 24 h. After the milling, a bright green suspension was obtained, which was diluted with toluene (2 mL) and used as-obtained or precipitated one time with acetonitrile (0.5 mL, 99.8%, Aldrich). The precipitate was redispersed in 2 mL toluene.

Alternatively, CsBr (0.011 g, 0.05 mmol, Aldrich, 99.9%) and PbBr₂ (0.018 g, 0.05 mmol) were loaded into a zirconia bowl with 25 zirconia balls (4 mm and 5 mm) and with 1.6 mL mesitylene and 0.01 g of OAmBr (0.03 mmol). The subsequent milling lasted 2 h at 500 rpm. The bright green crude solution was diluted with 2 mL toluene.

Mechanochemical synthesis of FAPbBr₃ NCs. Bulk FAPbBr₃ (0.02 g, 0.04 mmol, prepared as described) was loaded into a zirconia bowl with 25 zirconia balls (4 mm and 5 mm) and with OAmBr (0.01 g, 0.03 mmol) and 0.4 mL of mesitylene as the solvent. Other tested ligand systems were a mixture of OA (0.1 mL) and OLA (0.05 mL) and tetraoctylammonium bromide (0.01 g, Aldrich, 98%). The bowl was mounted on a planetary ball mill and the speed was set to 500 rpm. The milling time was varied from 30 min to 3 h. After the milling, a bright green suspension was obtained, which was diluted with toluene (2 mL) and used as is or precipitated one time with acetonitrile (0.5 mL). The precipitate was redispersed in 2 mL toluene.

Anion-exchange procedure. CsPbBr₃ NCs were prepared as described above. After the ball-milling experiment was completed, an additional 0.02 g OAmI (0.05 mmol) was added to the crude solution and the ball-milling experiment was continued for 1 h at 500 rpm. A bright-orange suspension was obtained.

Film preparation: Toluene solution of the perovskite NCs (10 mg/mL) was filtered using a 0.45 µm PTFE filter and drop-casted onto acetone/ethanol-cleaned glass slides.

Characterization. UV-Vis absorption spectra for the colloidal solutions were recorded using a Jasco V670 spectrometer in transmission mode. PL and absolute QY measurements were performed using a Fluorolog iHR 320 Horiba Jobin Yvon spectrofluorimeter equipped with a PMT detector, used to acquire steady-state PL spectra from solutions and films. QY values from NC dispersions were estimated according to the standard procedure using fluorescein as the

reference.⁷¹ Powder XRD patterns were recorded using a STOE STADI P powder diffractometer, operating in transmission mode. A germanium monochromator, Cu K α 1 irradiation, and a silicon strip detector, Dectris Mythen, were used. Transmission electron microscopy images were recorded using a Philips CM 12 microscope operating at 120 kV. Time-resolved PL measurements were performed using a time-correlated single-photon counting setup, equipped with an SPC-130-EM counting module (Becker & Hickl GmbH) and an IDQ-ID-100-20-ULN avalanche photodiode (Quantique) for recording the decay traces. The emission of the perovskite NCs was excited by a BDL-488-SMN laser (Becker & Hickl) with a pulse duration of 50 ps, wavelength of 488 nm, and CW power equivalent of ~0.5 mW, externally triggered at a 1 MHz repetition rate. PL emission from the samples was passed through a long-pass optical filter with an edge at 500 nm to reject the excitation laser line. Average radiative lifetimes were determined as: $\tau_{avg} = \frac{\sum_{i=1}^2 \tau_i^2 \cdot A_i}{\sum_{i=1}^2 \tau_i \cdot A_i}$, where A_i and τ_i are corresponding amplitudes and exponential decay parameters in biexponential analysis. PL QY measurements of the films were conducted using a method similar to that reported by Semonin *et al.*⁷² Using an integrating sphere (IS200-4, Thorlabs) with a short-pass filter (FES450, Thorlabs), the absorbance was corrected to reflectance and the scattering losses were estimated. A CW laser diode with a wavelength of 405 nm and a power of 0.2 W modulated at 30 Hz was used as the excitation source. The emitted light was measured using long-pass filters (FEL450, Thorlabs). The light intensity was measured by a broadband (0.1–20 μ m) UM9B-BL-DA pyroelectric photodetector (Gentec-EO). The modulated signal from the detector was recovered by a lock-in amplifier (SR 850, Stanford Research). The ratio between the emitted and absorbed light gave the energy yield. The PL QY was obtained from the value of the energy yield, corrected to the ratio of photon energies of the

1
2
3 laser beam and PL bands. The effect of emission re-absorption was taken into account in the
4
5 final calculation.
6
7
8
9

10 ASSOCIATED CONTENT

11
12
13
14 The Supporting Information is available free of charge on the ACS Publications website.
15
16 Additional photoluminescence spectra (PDF).
17
18

19 AUTHOR INFORMATION

20 21 **Corresponding Author**

22
23
24
25 *mvkovalenko@ethz.ch
26

27 **Present Addresses**

28
29
30 [‡]Massachusetts Institute of Technology, Department of Chemistry, 77 Massachusetts Ave,
31
32 Cambridge, MA 02139, USA
33
34

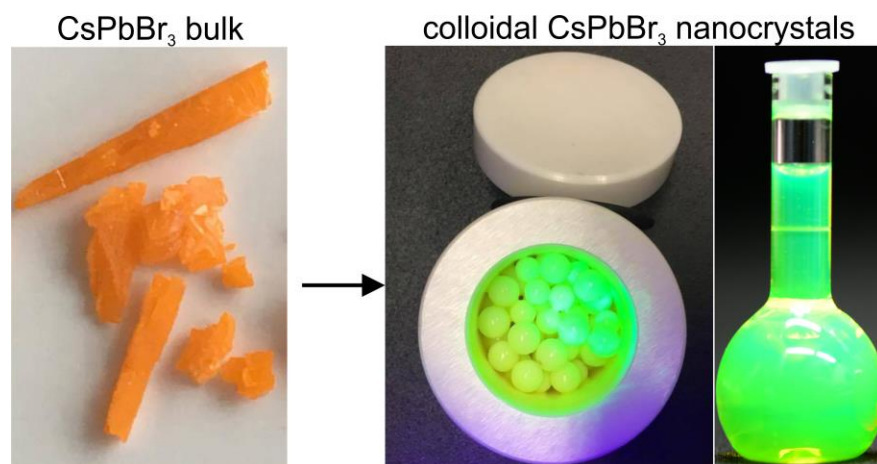
35 **Author Contributions**

36
37
38 All authors contributed to the writing of the manuscript and have given approval to the final
39
40 version of the manuscript.
41
42

43 ACKNOWLEDGMENTS

44
45
46 This work was financially supported by the European Union through the FP7 (ERC Starting
47
48 Grant NANOSOLID, GA No. 306733) and by the Swiss Federal Commission for Technology
49
50 and Innovation (CTI-No. 18614.1 PFNM-NM).
51
52
53
54
55
56
57
58
59
60

TOC



References:

- (1) Murray, C. B.; Norris, D. J.; Bawendi, M. G. Synthesis and Characterization of Nearly Monodisperse CdE (E = S, Se, Te) Semiconductor Nanocrystallites. *J. Am. Chem. Soc.* **1993**, *115*, 8706-8715.
- (2) Donegá, C. d. M.; Liljeroth, P.; Vanmaekelbergh, D. Physicochemical Evaluation of the Hot-Injection Method, a Synthesis Route for Monodisperse Nanocrystals. *Small* **2005**, *1*, 1152-1162.
- (3) Kwon, S. G.; Hyeon, T. Formation Mechanisms of Uniform Nanocrystals via Hot-Injection and Heat-Up Methods. *Small* **2011**, *7*, 2685-2702.
- (4) Kovalenko, M. V.; Manna, L.; Cabot, A.; Hens, Z.; Talapin, D. V.; Kagan, C. R.; Klimov, V. I.; Rogach, A. L.; Reiss, P.; Milliron, D. J.; Guyot-Sionnest, P.; Konstantatos, G.; Parak, W. J.; Hyeon, T.; Korgel, B. A.; Murray, C. B.; Heiss, W. Prospects of Nanoscience with Nanocrystals. *ACS Nano* **2015**, *9*, 1012-1057.
- (5) Hines, M. A.; Guyot-Sionnest, P. Synthesis and Characterization of Strongly Luminescing ZnS-Capped CdSe Nanocrystals. *J. Phys. Chem. B* **1996**, *100*, 468-471.
- (6) Beberwyck, B. J.; Alivisatos, A. P. Ion Exchange Synthesis of III-V Nanocrystals. *J. Am. Chem. Soc.* **2012**, *134*, 19977-19980.
- (7) Yarema, M.; Kovalenko, M. V. Colloidal Synthesis of InSb Nanocrystals with Controlled Polymorphism Using Indium and Antimony Amides. *Chem. Mater.* **2013**, *25*, 1788-1792.
- (8) Liu, W.; Chang, A. Y.; Schaller, R. D.; Talapin, D. V. Colloidal InSb Nanocrystals. *J. Am. Chem. Soc.* **2012**, *134*, 20258-20261.
- (9) Maurice, A.; Haro, M. L.; Hyot, B.; Reiss, P. Synthesis of Colloidal Indium Antimonide Nanocrystals Using Stibine. *Part. Part. Syst. Char.* **2013**, *30*, 828-831.
- (10) Cho, K. S.; Stokes, K. L.; Murray, C. B. Synthesis of PbSe, PbS, PbTe Nanocrystals (from Quantum Dots to Nanowires). *Abstr. Pap. Am. Chem. S.* **2003**, *225*, U74-U75.
- (11) Hines, M. A.; Scholes, G. D. Colloidal PbS Nanocrystals with Size-Tunable Near-Infrared Emission: Observation of Post-Synthesis Self-Narrowing of the Particle Size Distribution. *Adv. Mater.* **2003**, *15*, 1844-1849.

- (12) Cho, K.-S.; Talapin, D. V.; Gaschler, W.; Murray, C. B. Designing PbSe Nanowires and Nanorings Through Oriented Attachment of Nanoparticles. *J. Am. Chem. Soc.* **2005**, *127*, 7140-7147.
- (13) Murray, C. B.; Sun, S.; Gaschler, W.; Doyle, H.; Betley, T. A.; Kagan, C. R. Colloidal Synthesis of Nanocrystals and Nanocrystal Superlattices. *IBM J. Res. Dev.* **2001**, *45*, 47-56.
- (14) Wehrenberg, B. L.; Wang, C.; Guyot-Sionnest, P. Interband and Intraband Optical Studies of PbSe Colloidal Quantum Dots. *J. Phys. Chem. B* **2002**, *106*, 10634-10640.
- (15) Kovalenko, M. V.; Talapin, D. V.; Loi, M. A.; Cordella, F.; Hesser, G.; Bodnarchuk, M. I.; Heiss, W. Quasi-Seeded Growth of Ligand-Tailored PbSe Nanocrystals through Cation-Exchange-Mediated Nucleation. *Angew. Chem. Int. Edit* **2008**, *47*, 3029-3033.
- (16) Murphy, J. E.; Beard, M. C.; Norman, A. G.; Ahrenkiel, S. P.; Johnson, J. C.; Yu, P. R.; Micic, O. I.; Ellingson, R. J.; Nozik, A. J. PbTe Colloidal Nanocrystals: Synthesis, Characterization, and Multiple Exciton Generation. *J. Am. Chem. Soc.* **2006**, *128*, 3241-3247.
- (17) Lambert, K.; De Geyter, B.; Moreels, I.; Hens, Z. PbTeCdTe CoreShell Particles by Cation Exchange, a HR-TEM study. *Chem. Mater.* **2009**, *21*, 778-780.
- (18) Lu, W. G.; Fang, J. Y.; Stokes, K. L.; Lin, J. Shape Evolution and Self-assembly of Monodisperse PbTe Nanocrystals. *J. Am. Chem. Soc.* **2004**, *126*, 11798-11799.
- (19) Urban, J. J.; Talapin, D. V.; Shevchenko, E. V.; Murray, C. B. Self-Assembly of PbTe Quantum Dots into Nanocrystal Superlattices and Glassy Films. *J. Am. Chem. Soc.* **2006**, *128*, 3248-3255.
- (20) Xu, X.; Hu, L.; Gao, N.; Liu, S.; Wageh, S.; Al-Ghamdi, A. A.; Alshahrie, A.; Fang, X. Controlled Growth from ZnS Nanoparticles to ZnS–CdS Nanoparticle Hybrids with Enhanced Photoactivity. *Adv. Funct. Mater.* **2015**, *25*, 445-454.
- (21) Kovalenko, M. V.; Schaller, R. D.; Jarzab, D.; Loi, M. A.; Talapin, D. V. Inorganically Functionalized PbS–CdS Colloidal Nanocrystals: Integration into Amorphous Chalcogenide Glass and Luminescent Properties. *J. Am. Chem. Soc.* **2012**, *134*, 2457-2460.
- (22) Pietryga, J. M.; Schaller, R. D.; Werder, D.; Stewart, M. H.; Klimov, V. I.; Hollingsworth, J. A. Pushing the Band Gap Envelope: Mid-Infrared Emitting Colloidal PbSe Quantum Dots. *J. Am. Chem. Soc.* **2004**, *126*, 11752-11753.
- (23) Schaller, R.; Petruska, M.; Klimov, V. Tunable Near-Infrared Optical Gain and Amplified Spontaneous Emission Using PbSe Nanocrystals. *J. Phys. Chem. B* **2003**, *107*, 13765-13768.
- (24) Barnard, A. S.; Xu, H.; Li, X.; Pradhan, N.; Peng, X. Modelling the Formation of High Aspect CdSe Quantum Wires: Axial-Growth Versus Oriented-Attachment Mechanisms. *Nanotechnology* **2006**, *17*, 5707-5714.
- (25) Li, Z.; Peng, X. Size/Shape-Controlled Synthesis of Colloidal CdSe Quantum Disks: Ligand and Temperature Effects. *J. Am. Chem. Soc.* **2011**, *133*, 6578-6586.
- (26) Ithurria, S.; Tessier, M. D.; Mahler, B.; Lobo, R. P. S. M.; Dubertret, B.; Efros, A. L. Colloidal Nanoplatelets With Two-Dimensional Electronic Structure. *Nat. Mater.* **2011**, *10*, 936-941.
- (27) Talapin, D. V.; Nelson, J. H.; Shevchenko, E. V.; Aloni, S.; Sadtler, B.; Alivisatos, A. P. Seeded Growth of Highly Luminescent CdSe/CdS Nanoheterostructures with Rod and Tetrapod Morphologies. *Nano Lett.* **2007**, *7*, 2951-2959.
- (28) Kovalenko, M. V.; Protesescu, L.; Bodnarchuk, M. I. Properties and Potential Optoelectronic Applications of Lead Halide Perovskite Nanocrystals. *Science* **2017**, *358*, 745-750.

- (29) Protesescu, L.; Yakunin, S.; Bodnarchuk, M. I.; Krieg, F.; Caputo, R.; Hendon, C. H.; Yang, R. X.; Walsh, A.; Kovalenko, M. V. Nanocrystals of Cesium Lead Halide Perovskites (CsPbX_3 , X = Cl, Br, and I): Novel Optoelectronic Materials Showing Bright Emission with Wide Color Gamut. *Nano Lett.* **2015**, *15*, 3692-3696.
- (30) Vybornyi, O.; Yakunin, S.; Kovalenko, M. V. Polar-Solvent-Free Colloidal Synthesis of Highly Luminescent Alkylammonium Lead Halide Perovskite Nanocrystals. *Nanoscale* **2016**, *8*, 6278-6283.
- (31) Protesescu, L.; Yakunin, S.; Bodnarchuk, M. I.; Bertolotti, F.; Masciocchi, N.; Guagliardi, A.; Kovalenko, M. V. Monodisperse Formamidinium Lead Bromide Nanocrystals with Bright and Stable Green Photoluminescence. *J. Am. Chem. Soc.* **2016**, *138*, 14202-14205.
- (32) Nedelcu, G.; Protesescu, L.; Yakunin, S.; Bodnarchuk, M. I.; Grotevent, M. J.; Kovalenko, M. V. Fast Anion-Exchange in Highly Luminescent Nanocrystals of Cesium Lead Halide Perovskites (CsPbX_3 , X = Cl, Br, I). *Nano Lett.* **2015**, *15*, 5635-5640.
- (33) Schmidt, L. C.; Pertegás, A.; González-Carrero, S.; Malinkiewicz, O.; Agouram, S.; Mínguez Espallargas, G.; Bolink, H. J.; Galian, R. E.; Pérez-Prieto, J. Nontemplate Synthesis of $\text{CH}_3\text{NH}_3\text{PbBr}_3$ Perovskite Nanoparticles. *J. Am. Chem. Soc.* **2014**, *136*, 850-853.
- (34) Sichert, J. A.; Tong, Y.; Mutz, N.; Vollmer, M.; Fischer, S.; Milowska, K. Z.; García Cortadella, R.; Nickel, B.; Cardenas-Daw, C.; Stolarczyk, J. K.; Urban, A. S.; Feldmann, J. Quantum Size Effect in Organometal Halide Perovskite Nanoplatelets. *Nano Lett.* **2015**, *15*, 6521-6527.
- (35) Bekenstein, Y.; Koscher, B. A.; Eaton, S. W.; Yang, P.; Alivisatos, A. P. Highly Luminescent Colloidal Nanoplates of Perovskite Cesium Lead Halide and Their Oriented Assemblies. *J. Am. Chem. Soc.* **2015**, *137*, 16008-16011.
- (36) Akkerman, Q. A.; Motti, S. G.; Srimath Kandada, A. R.; Mosconi, E.; D'Innocenzo, V.; Bertoni, G.; Marras, S.; Kamino, B. A.; Miranda, L.; De Angelis, F.; Petrozza, A.; Prato, M.; Manna, L. Solution Synthesis Approach to Colloidal Cesium Lead Halide Perovskite Nanoplatelets with Monolayer-Level Thickness Control. *J. Am. Chem. Soc.* **2016**, *138*, 1010-1016.
- (37) Weidman, M. C.; Goodman, A. J.; Tisdale, W. A. Colloidal Halide Perovskite Nanoplatelets: An Exciting New Class of Semiconductor Nanomaterials. *Chem. Mater.* **2017**, *29*, 5019-5030.
- (38) Suryanarayana, C. Mechanical Alloying and Milling. *Prog. Mater. Sci.* **2001**, *46*, 1-184.
- (39) Bonetti, E.; Del Bianco, L.; Signoretti, S.; Tiberto, P. Synthesis by Ball Milling and Characterization of Nanocrystalline Fe_3O_4 and $\text{Fe}/\text{Fe}_3\text{O}_4$ Composite System. *J. App. Phys.* **2001**, *89*, 1806-1815.
- (40) Grisorio, R.; De Marco, L.; Baldisserrri, C.; Martina, F.; Serantoni, M.; Gigli, G.; Suranna, G. P. Sustainability of Organic Dye-Sensitized Solar Cells: The Role of Chemical Synthesis. *ACS Sustain. Chem. Eng.* **2015**, *3*, 770-777.
- (41) Oleszak, D.; Matyja, H. Nanocrystalline Fe-Based Alloys Obtained by Mechanical Alloying. *Nanostruct. Mater.* **1995**, *6*, 425-428.
- (42) Salah, N.; Habib, S. S.; Khan, Z. H.; Memic, A.; Azam, A.; Alarfaj, E.; Zahed, N.; Al-Hamedi, S. High-Energy Ball Milling Technique for ZnO Nanoparticles as Antibacterial Material. *Int. J. Nanomed.* **2011**, *6*, 863-869.
- (43) Han, Q.; Setchi, R.; Evans, S. L. Synthesis and Characterisation of Advanced Ball-Milled $\text{Al}-\text{Al}_2\text{O}_3$ Nanocomposites for Selective Laser Melting. *Powder Technol.* **2016**, *297*, 183-192.
- (44) Yi, M.; Shen, Z. A Review on Mechanical Exfoliation for the Scalable Production of Graphene. *J. Mater. Chem. A* **2015**, *3*, 11700-11715.

- (45) Urbieto, A.; Fernández, P.; Piqueras, J. Study of Structure and Luminescence of CdSe Nanocrystals Obtained by Ball Milling. *J. App. Phys.* **2004**, *96*, 2210.
- (46) Tan, G. L.; Hömmerich, U.; Temple, D.; Wu, N. Q.; Zheng, J. G.; Loutts, G. Synthesis and Optical Characterization of CdTe Nanocrystals Prepared by Ball Milling Process. *Scripta Mater.* **2003**, *48*, 1469-1474.
- (47) Kang, J.; Wang, L.-W. High Defect Tolerance in Lead Halide Perovskite CsPbBr₃. *J. Phys. Chem. Lett.* **2017**, *8*, 489-493.
- (48) Guo, Y.; Wang, Q.; Saidi, W. A. Structural Stabilities and Electronic Properties of High-Angle Grain Boundaries in Perovskite Cesium Lead Halides. *J. Phys. Chem. C* **2017**, *121*, 1715-1722.
- (49) ten Brinck, S.; Infante, I. Surface Termination, Morphology, and Bright Photoluminescence of Cesium Lead Halide Perovskite Nanocrystals. *ACS Energy Lett.* **2016**, *1*, 1266-1272.
- (50) Zhu, Z.-Y.; Yang, Q.-Q.; Gao, L.-F.; Zhang, L.; Shi, A.-Y.; Sun, C.-L.; Wang, Q.; Zhang, H.-L. Solvent-Free Mechanochemical Synthesis of Composition-Tunable Cesium Lead Halide Perovskite Quantum Dots. *J. Phys. Chem. Lett.* **2017**, *8*, 1610-1614.
- (51) Manukyan, K. V.; Yeghishyan, A. V.; Moskovskikh, D. O.; Kapaldo, J.; Mintairov, A.; Mukasyan, A. S. Mechanochemical Synthesis of Methylammonium Lead Iodide Perovskite. *J. Mater. Sci.* **2016**, *51*, 9123-9130.
- (52) Jang, D. M.; Kim, D. H.; Park, K.; Park, J.; Lee, J. W.; Song, J. K. Ultrasound Synthesis Of Lead Halide Perovskite Nanocrystals. *J. Mater. Chem. C* **2016**, *4*, 10625-10629.
- (53) Pan, Q.; Hu, H.; Zou, Y.; Chen, M.; Wu, L.; Yang, D.; Yuan, X.; Fan, J.; Sun, B.; Zhang, Q. Microwave-Assisted Synthesis Of High-Quality "All-Inorganic" CsPbX₃ (X = Cl, Br, I) Perovskite Nanocrystals and Their Application in Light Emitting Diodes. *J. Mater. Chem. C* **2017**, *5*, 10947-10954.
- (54) Long, Z.; Ren, H.; Sun, J.; Ouyang, J.; Na, N. High-Throughput and Tunable Synthesis of Colloidal CsPbX₃ Perovskite Nanocrystals in a Heterogeneous System by Microwave Irradiation. *Chem. Commun.* **2017**, *53*, 9914-9917.
- (55) Dirin, D. N.; Protesescu, L.; Trummer, D.; Kochetygov, I. V.; Yakunin, S.; Krumeich, F.; Stadie, N. P.; Kovalenko, M. V. Harnessing Defect-Tolerance at the Nanoscale: Highly Luminescent Lead Halide Perovskite Nanocrystals in Mesoporous Silica Matrixes. *Nano Lett.* **2016**, *16*, 5866-5874.
- (56) Lignos, I.; Stavrakis, S.; Nedelcu, G.; Protesescu, L.; deMello, A. J.; Kovalenko, M. V. Synthesis of Cesium Lead Halide Perovskite Nanocrystals in a Droplet-Based Microfluidic Platform: Fast Parametric Space Mapping. *Nano Lett.* **2016**, *16*, 1869-1877.
- (57) Tan, Y.; Zou, Y.; Wu, L.; Huang, Q.; Yang, D.; Chen, M.; Ban, M.; Wu, C.; Wu, T.; Bai, S.; Song, T.; Zhang, Q.; Sun, B. Highly Luminescent and Stable Perovskite Nanocrystals with Octylphosphonic Acid as a Ligand for Efficient Light-Emitting Diodes. *ACS Appl. Mater. Interfaces* **2018**, *10*, 3784-3792.
- (58) Krieg, F.; Ochsenbein, S.; Yakunin, S.; ten Brinck, S.; Aellen, P.; Süess, A.; Clerc, B.; Guggisberg, D.; Nazarenko, O.; Shynkarenko, Y.; Kumar, S.; Shih, C.-J.; Infante, I.; Kovalenko, M. V. Colloidal CsPbX₃ (X=Cl, Br, I) Nanocrystals 2.0: Zwitterionic Capping Ligands for Improved Durability and Stability. *ACS Energy Lett.* **2018**.
- (59) Sun, S.; Yuan, D.; Xu, Y.; Wang, A.; Deng, Z. Ligand-Mediated Synthesis of Shape-Controlled Cesium Lead Halide Perovskite Nanocrystals via Reprecipitation Process at Room Temperature. *ACS Nano* **2016**, *10*, 3648-3657.

- (60) Aygüler, M. F.; Weber, M. D.; Puscher, B. M. D.; Medina, D. D.; Docampo, P.; Costa, R. D. Light-Emitting Electrochemical Cells Based on Hybrid Lead Halide Perovskite Nanoparticles. *J. Phys. Chem. C* **2015**, *119*, 12047-12054.
- (61) Liu, H.; Wu, Z.; Gao, H.; Shao, J.; Zou, H.; Yao, D.; Liu, Y.; Zhang, H.; Yang, B. One-Step Preparation of Cesium Lead Halide CsPbX₃ (X = Cl, Br, and I) Perovskite Nanocrystals by Microwave Irradiation. *ACS Appl. Mater. Interfaces* **2017**, *9*, 42919-42927.
- (62) Elseman, A. M.; Rashad, M. M.; Hassan, A. M. Easily Attainable, Efficient Solar Cell with Mass Yield of Nanorod Single-Crystalline Organo-Metal Halide Perovskite Based on a Ball Milling Technique. *ACS Sustain. Chem. Eng.* **2016**, *4*, 4875-4886.
- (63) De Roo, J.; Ibáñez, M.; Geiregat, P.; Nedelcu, G.; Walravens, W.; Maes, J.; Martins, J. C.; Van Driessche, I.; Kovalenko, M. V.; Hens, Z. Highly Dynamic Ligand Binding and Light Absorption Coefficient of Cesium Lead Bromide Perovskite Nanocrystals. *ACS Nano* **2016**, *10*, 2071-2081.
- (64) Giansante, C.; Infante, I. Surface Traps in Colloidal Quantum Dots: A Combined Experimental and Theoretical Perspective. *J. Phys. Chem. Lett.* **2017**, *8*, 5209-5215.
- (65) Chin, Z. H.; Perng, T. P. In Situ Observation of Combustion to Form Tin During Ball Milling Ti in Nitrogen. *Appl. Phys. Lett.* **1997**, *70*, 2380-2382.
- (66) Lv, Y.-J.; Su, J.; Long, Y.-F.; Cui, X.-R.; Lv, X.-Y.; Wen, Y.-X. Effects of Ball-to-Powder Weight Ratio on the Performance of LiFePO₄/C Prepared by Wet-Milling Assisted Carbothermal Reduction. *Powder Technol.* **2014**, *253*, 467-473.
- (67) Alarousu, E.; El-Zohry, A. M.; Yin, J.; Zhumeckenov, A. A.; Yang, C.; Alhabshi, E.; Gereige, I.; AlSaggaf, A.; Malko, A. V.; Bakr, O. M.; Mohammed, O. F. Ultralong Radiative States in Hybrid Perovskite Crystals: Compositions for Submillimeter Diffusion Lengths. *J. Phys. Chem. Lett.* **2017**, *8*, 4386-4390.
- (68) Koscher, B. A.; Swabeck, J. K.; Bronstein, N. D.; Alivisatos, A. P. Essentially Trap-Free CsPbBr₃ Colloidal Nanocrystals by Postsynthetic Thiocyanate Surface Treatment. *J. Am. Chem. Soc.* **2017**, *139*, 6566-6569.
- (69) Dirin, D. N.; Cherniukh, I.; Yakunin, S.; Shynkarenko, Y.; Kovalenko, M. V. Solution-Grown CsPbBr₃ Perovskite Single Crystals for Photon Detection. *Chem. Mater.* **2016**, *28*, 8470-8474.
- (70) Nie, W.; Tsai, H.; Asadpour, R.; Blancon, J.-C.; Neukirch, A. J.; Gupta, G.; Crochet, J. J.; Chhowalla, M.; Tretiak, S.; Alam, M. A.; Wang, H.-L.; Mohite, A. D. High-Efficiency Solution-Processed Perovskite Solar Cells with Millimeter-Scale Grains. *Science* **2015**, *347*, 522-525.
- (71) Grabolle, M.; Spieles, M.; Lesnyak, V.; Gaponik, N.; Eychmüller, A.; Resch-Genger, U. Determination of the Fluorescence Quantum Yield of Quantum Dots: Suitable Procedures and Achievable Uncertainties. *Anal. Chem.* **2009**, *81*, 6285-6294.
- (72) Semonin, O. E.; Johnson, J. C.; Luther, J. M.; Midgett, A. G.; Nozik, A. J.; Beard, M. C. Absolute Photoluminescence Quantum Yields of IR-26 Dye, PbS, and PbSe Quantum Dots. *J. Phys. Chem. Lett.* **2010**, *1*, 2445-2450.